Geological Survey of Japan Cruise Report No. 23, p. 165-185, 1994

IX. MINERALOGY, GEOCHEMISTRY AND INTERNAL GROWTH STRUCTURE OF MANGANESE NODULES IN THE WESTERN PART OF THE PENRHYN BASIN, SOUTH PACIFIC (GH83-3 AREA)

Akira Usui and Naoki Mita

Introduction

As reported by earlier workers, mineralogical and chemical composition is one of the most important criteria to discriminate origins of marine ferromanganese deposits in the ocean. The deposits are composed in principle of three mineral components: hydrogenetic vernadite, diagenetic buserite, and hydrothermal todorokite (Burns *et al.*, 1983; Stouff and Boulègue, 1988; Usui *et al.*, 1989). The minerals are often intergrown on a microscopic or submicroscopical scale in nodules, crusts, sediments etc. Furthermore, the composition of minerals itself considerably fluctuates around their stoichiometric composition and some are continuous series. Bulk and layer-by-layer analyses are thus most practical methods in characterizing marine manganese deposits.

In this paper, nodules and crusts are chemically and mineralogically described in terms of regional, local, and intra-nodule compositional variation for the purpose of understanding conditions and processes of the ferromanganese deposit in the Penrhyn Basin which proved to be a typical slowly-grown hydrogenetic deposits.

Samples and Methods

Nodule samples were split after morphological description for chemical analysis, ore microscopy, scanning microscopy (SEM), powder X-ray diffraction (XRD), and radiochemical dating. The procedures of analysis are show in a flow diagram (Fig. IX-1). Described nodules were split and polished for ore microscopy, one half was ground into powder and divided into three parts for X-ray powder diffraction analysis, chemical analysis, and water content determination. The 169 powders were prepared from 90 stations in order to describe the regional and local variations of bulk chemical composition and the layer-by-layer variation inside nodules. About 80 powders were made from a half to several entire nodules so that they may represent approximate mean bulk characteristics. Some nodules were divided into 2 to 10-mm thick layers from nodule surface to nuclei. Nine elements (Mn, Fe, Cu, Ni, Co, Pb, Zn, Si, and Al) were determined by atomic absorption spectroscopy (AA) according

Keywords: manganese nodule, chemical composition, mineral composition, morphology, internal structure, sedimentary condition, growth history, Manihiki Plateau, Hakurei-Maru, Penrhyn Basin

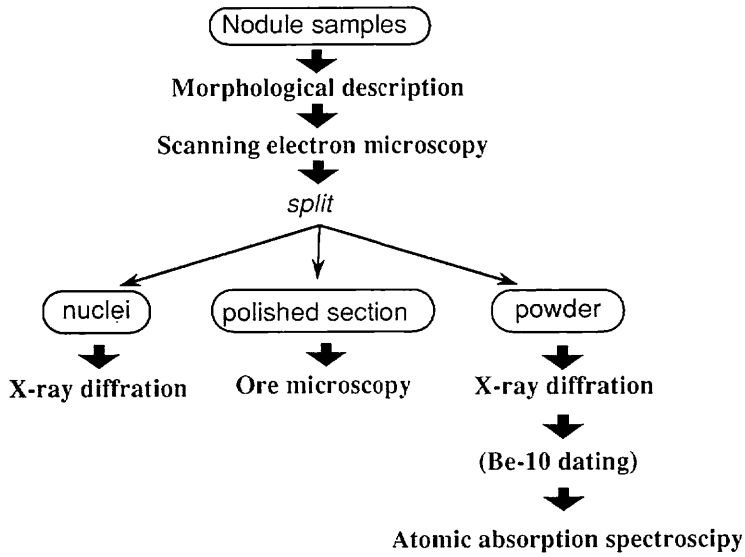

Fig. IX-1 Method of analysis of manganese nodules of GH83-3 area.

to analytical guideline of GSJ (Terashima, 1978; Mochizuki and Terashima, 1983). Water contents were determined as H_2O+ by Penfield Method and H_2O- by drying in oven.

Mineral composition was determined by XRD and/or microscopy for air-dried powders. XRD was accomplished for the same powder samples of AA in a constant analysis condition by using a diffractometer Type RAD-rA (Rigaku Denki Co. Ltd.). Peak heights were measured at 10 and 2.4 Å d-spacings for semi-quantitative estimation of ferromanganese minerals; 10 and 5 Å d-spacings are diagnostic of buserite, but 2.4 Å and 1.4 Å reflections are responsible both to buserite and vernadite. Accessory silicate minerals, phosphates, carbonates etc. were examined and estimated in comparison with ASTM and JCPDS data files.

Microscopic identification was also available in identifying ferromanganese minerals and for description of internal microstructure. The criteria for mineral identification follows after Usui (1979a) and Usui *et al.* (1989).

Chemical composition and semiquantitative mineral contents are listed in Appendix IX-1 together with simplified description.

Mineralogy of ferromanganese deposits.

The structural characterization of marine manganese minerals is still controversial, due to their low crystallinity, submicroscopical size, and hydrous nature (Burns and Burns, 1977; Giovanoli, 1980; Burns *et al.*, 1983; Ostwald, 1984). Terminology is complicated in literatures. In this article, the mineral terms *todorokite*, *buserite*, and *vernadite* are used. The former two minerals, which are both 10 Å manganates, are practically distinguishable by thermal treatment at 110°C in air (Usui *et al.*, 1989). Semi-quantitative XRD analysis shows that only vernadite is the principal ferromanganese mineral of GH83-3 nodules (Appendix IX-1), and buserite is a minor compo-

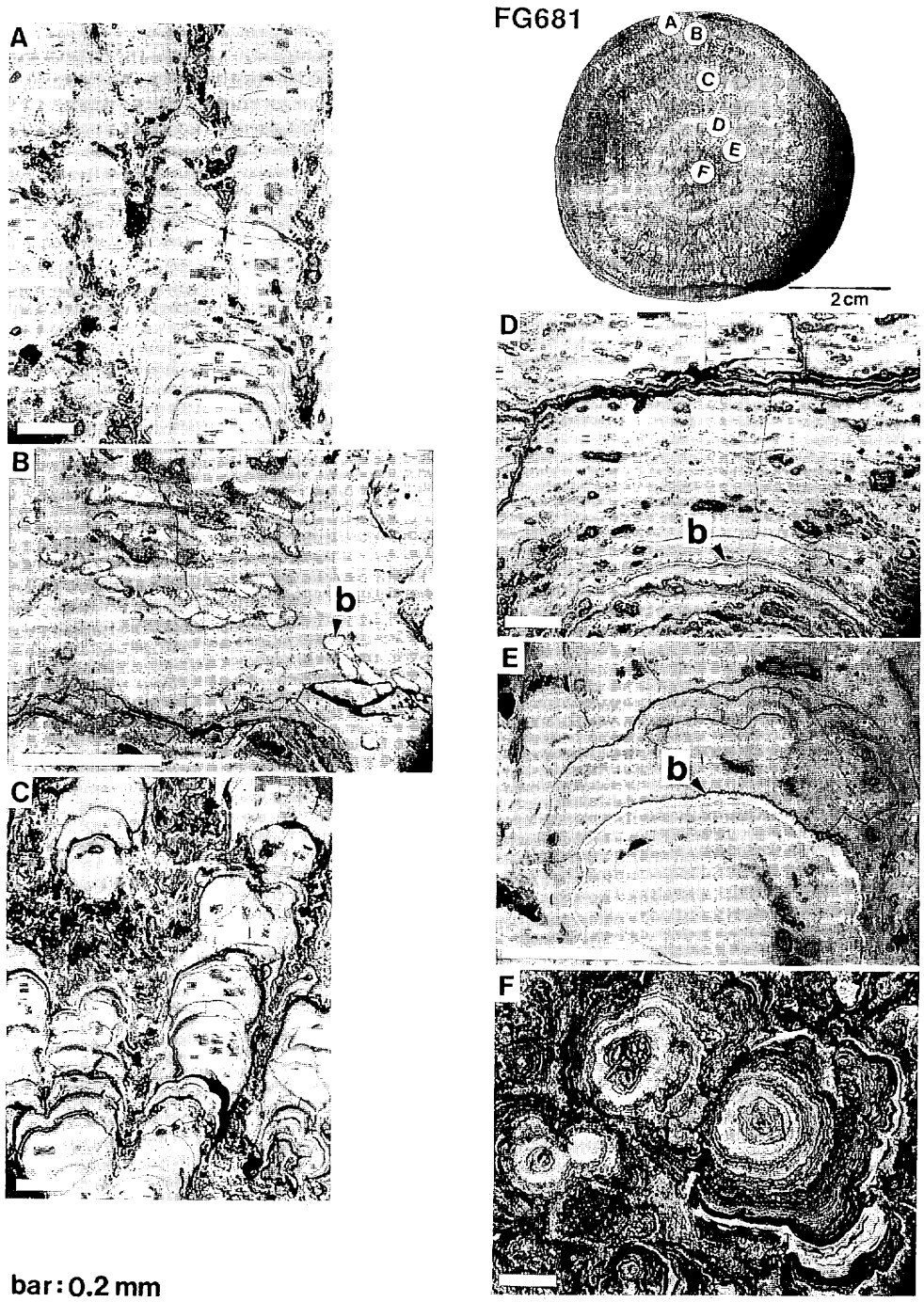

Fig. IX-2 Stratigraphic change of microstructure inside a manganese nodule. A) dense columer structure, B) void filling buserite, C) sparse columnar structure, D) stratification, E) lamination, F) concentric lamination. Bright area of marked "b" in photos is buserite, and other gray part is vernadite.

Table IX-1 Comparison of element concentration of GH83-3 hydrogenetic nodules with other hydrogenetic ferromanganese deposits in the Pacific.

	Nodules		Crusts	
	GH83-3 (bulk) this study	type s (GH82-4) Usui & Mita (1992)	Hawaii Ridge Hein et al. (1987)	Johnstone Is. Hein et al. (1987)
n	*147*	*67*	*15*	*40*
Mn (%)	17.3	21.7	21.0	22.0
Fe (%)	16.1	13.3	18.0	17.0
Mn/Fe	1.20	1.70	1.13	1.23
Cu (%)	0.22	0.60	0.10	0.11
Ni (%)	0.43	0.79	0.37	0.43
Co (%)	0.42	0.20	0.60	0.70
Pb (%)	0.084	0.046	0.180	0.170
Si (%)	7.0	8.6	10.3	7.7

nent. Only one exception is the occurrence of hydrothermal todorokite (heat-resistant) in nucleus of FG692 nodules. Buserite is detectable on XRD diagrams in some samples but its bulk content is mostly less than several percent, as revealed by microscopical observations. On polished sections, buserite occurs occasionally as thin concordant layers, replacement of biogenic structure, or filling of voids or veins (Fig. IX-2) inside the nodules not on the recent surface of nodules. The 7 Å mineral (so-called *birnessite*) was not detected from any nodules from this area.

Manganese-free accessory minerals in the nodules are quartz, plagioclase, phillipsite, and smectite. Quartz and phillipsite are dominant, but plagioclases and smectite are less dominant. Silicate minerals occur as fine particles within oxide layers or as nuclei and inclusions. As shown in a later section, soft, fragile and porous nodules of 1 to 2 cm diameter are distinguishable on polished sections as old grown part at the center of large nodules (Facies B: see Chapter VIII). The inner old nodules are enriched in smectite and often in quartz, but lacking phillipsite. The nodules are markedly similar in minor minerals to those soft nodules in Unit II buried in piston cores.

Chemistry of ferromanganese deposits.

The bulk chemical composition of the GH83-3 nodules is characterized by low Mn/Fe ratio, Cu, Ni, Zn and high Co and Pb, which are common feature of hydrogenetic nodules and crusts. As compared with hydrogenetic nodules of the Central Pacific Basin (type s in the GH82-4 area), this tendency is more prominent. The general characteristics is more similar to manganese crusts on Pacific seamounts rather than hydrogenetic nodules on the sea floor which are more affected by early diagenetic processes on the sea floor (Table IX-1).

Buserite is the major host phase of Cu, Ni and Zn in nodules which are accumulated by early diagenetic processes of surface pelagic sediments. As markedly shown in Figure IX-3, concentrations of the elements are linearly correlated with peak height of buserite at 10 Å d-spacing on XRD charts. The ternary diagram Mn-Fe-(Cu+Ni+Zn) also demonstrate that the GH83-3 nodules are composed mainly of hydrogenetic

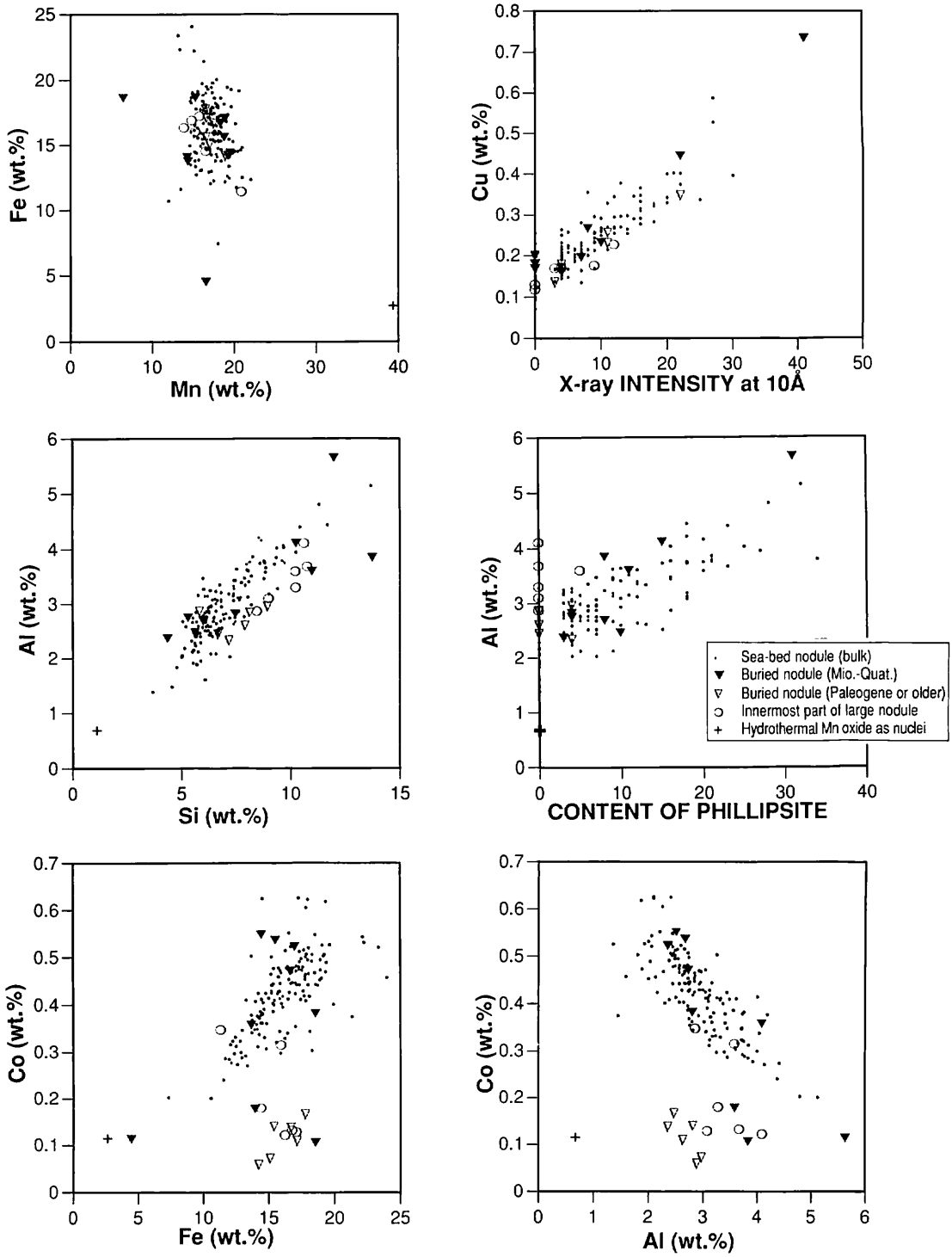

Fig. IX-3 Correlation plots for element concentrations and mineral contents. Mineral content is expressed in relative scales. Legend is the same in Table IX-3.

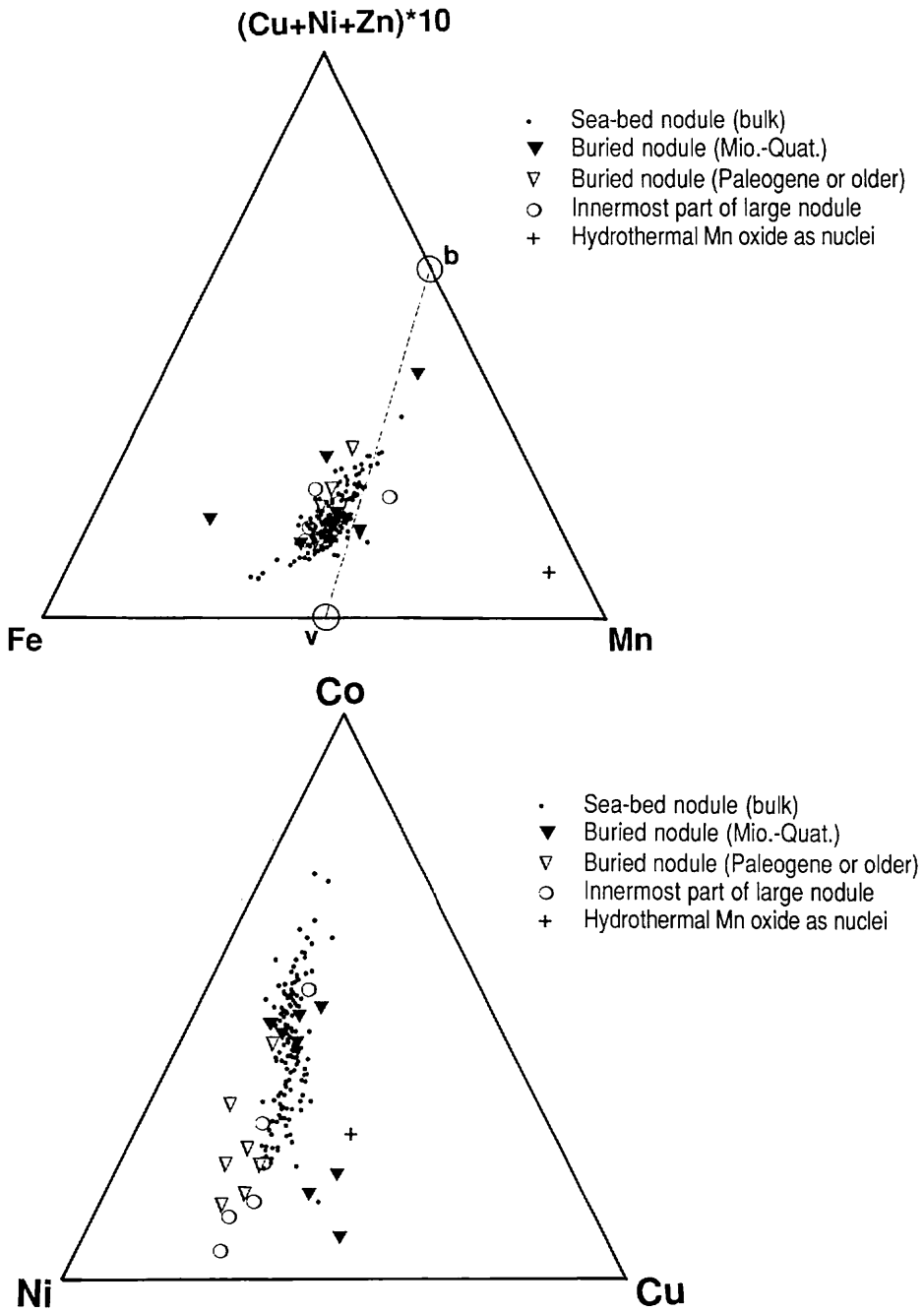

Fig. IX-4 Ternary diagrams of element concentration ratios Mn/Fe/(Cu+Ni+Zn) and Cu/Ni/Co. "b" and "v" in the upper diagram denote ideal compositions of buserite and vernadite. Legend is the same as in Table IX-3.

Table IX-2 Correlation matrix between 13 metallic elements for 147 sea-bed nodules. Only the correlation coefficients of which absolute value exceed 0.5 are noted. Other symbols, +, −, and * in the matrix mean the coefficients between +0.5 and+0.3, between −0.5 and −0.3, and ±0.3, respectively.

Mn	Zn	Ni	Cu	Fe	Co	Pb	Si	Al	Na	K	Ca	Mg	
1	0.47	+	+	*	*	*	-	*	*	*	+	+	Mn
	1	0.86	0.79	-	-	-	*	+	*	*	*	0.87	Zn
		1	0.91	-0.78	-0.60	-	+	0.61	+	+	*	0.91	Ni
			1	-0.75	-0.69	-	+	0.68	+	+	-	0.87	Cu
				1	0.69	0.64	-0.62	-0.81	-0.66	-0.72	*	-0.67	Fe
					1	+	-0.64	-0.78	-	-0.71	+	-0.65	Co
						1	-	-	-	-	*	-	Pb
							1	0.86	0.78	0.90	-	+	Si
								1	0.73	0.88	-	0.63	Al
									1	0.85	*	+	Na
										1	-	+	K
											1	-	Ca
												1	Mg

vernadite and minor buserite (Fig. IX-4). As shown by microscopical observations, buserite does not form recent surfaces of nodules, but develops inside the nodules as older layers. The correlation coefficients for elements in sea-bed nodules (n=147) distinguish three phases (Table IX-2). The hydrogenetic vernadite which accommodate Fe, Mn, Co and Pb; the diagenetic buserite with Mn, Cu, Ni and Zn; and detrital aluminosilicate minerals with Na, K and Mg. Ca is not significantly related with any elements.

Minor intra-nodule variation is seen between top (sea water side) and bottom (sediment side) of large flattened nodules. Cu, Ni, Zn are slightly more enriched in bottom sides, while Co is enriched in top sides. Likewise smaller nodules tend to contain more buserite than larger nodules in a single site probably influenced by week diagenetic process at surface sediments.

The most marked intra-nodule compositional difference is the Co concentration found between younger generations (approximately 1 to 3 cm depths from surface) and innermost old soft nodules. In many of large nodules, Co concentration decreases from 0.5-0.6 wt.% at the surface to 0.1 wt.% at the center (Fig. IX-5).

Comparison of sea-bed nodules and buried nodules in cores

Among 17 piston cores, 8 buried nodules occur within 10 sediment cores. The nodule deposit is not altogether strata-bound deposits, but their occurrence are spread over various horizons even in the same core. Nishimura and Saito (Chapter IV of this volume) found a long-term hiatus between Unit I (Recent to late Miocene) and Unit II (Oligocene to Cretaceous). The buried nodules occur both within Units I and II (Fig. VIII-14).

Nodules in Unit II are typically soft, fragile, and porous. The diameter ranges 1 to 2.5 cm, and their surface often have submetallic silver sheen. These characteristics are unique to Unit II nodules. In contrast, the nodules in Unit I are similar in appearance to seabed nodules, but are smaller in size.

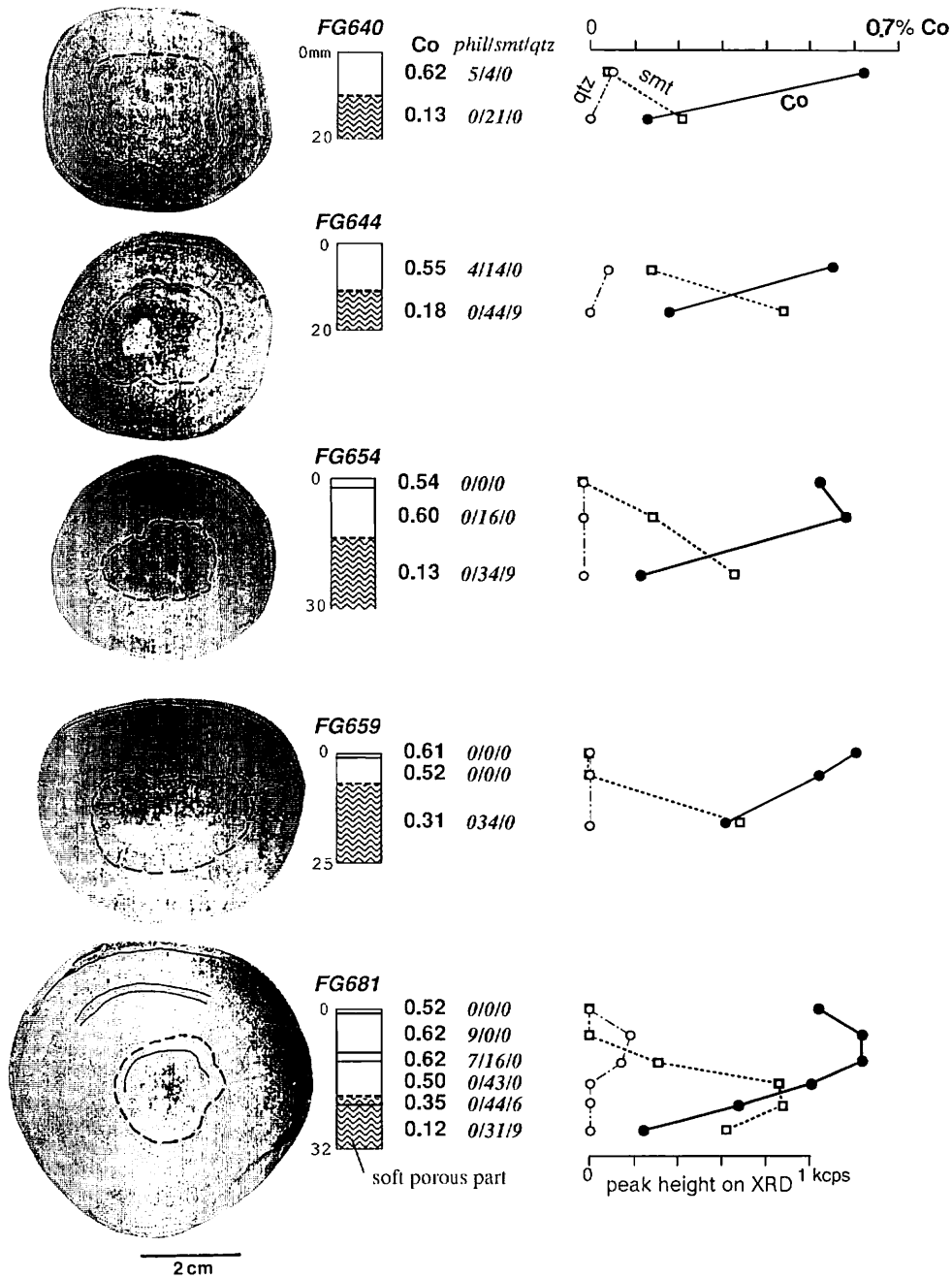

Fig. IX-5 Photographs of nodule sections under reflecting lights, schematic stratigraphy of nodules, and significant variations of Co and mineral contents.

Table IX-3 Comparison of element concentrations between sea-bed nodules, buried nodules, internal old nodules, and hydrothermal deposits in GH83-3 area.

		Mn				Fe				Cu				Ni				Co			
	n	ave.	s.d.	max.	min.	ave.	s.d.	max.	min.	ave.	s.d.	max.	min.	ave.	s.d.	max.	min.	ave.	s.d.	max.	min.
total	169	17.3	2.6	39.4	6.4	15.9	2.8	24.0	2.6	0.22	0.09	0.73	0.07	0.43	0.14	0.93	0.13	0.40	0.11	0.62	0.06
sea-bed(bulk)	147	17.3	1.7	22.1	12.1	16.1	2.5	24.0	7.3	0.22	0.08	0.58	0.07	0.43	0.13	0.81	0.13	0.42	0.08	0.62	0.20
buried (Unit I)	9	15.9	4.1	19.6	6.4	14.8	4.3	18.6	4.5	0.28	0.19	0.73	0.16	0.42	0.17	0.75	0.23	0.36	0.18	0.55	0.10
buried (Unit II)	6	17.3	0.9	19.0	16.6	16.1	1.4	17.8	14.2	0.22	0.08	0.35	0.14	0.53	0.22	0.93	0.31	0.12	0.04	0.17	0.06
sea-bed (inside)	6	16.3	2.5	21.0	14.0	15.3	2.2	17.1	11.3	0.16	0.04	0.22	0.12	0.47	0.16	0.66	0.30	0.20	0.10	0.35	0.12
hydrothermal	1	39.4	-	39.4	39.4	2.6	-	2.6	2.6	0.17	-	0.17	0.17	0.16	-	0.16	0.16	0.11	-	0.11	0.11

		Si				Al				Zn				Pb				Ca			
total	169	7.13	1.76	13.74	1.11	2.93	0.68	5.63	0.67	0.059	0.011	0.122	0.035	0.080	0.027	0.208	0.002	1.93	0.28	3.16	0.91
sea-bed(bulk)	147	6.97	1.47	13.68	3.69	2.91	0.64	5.12	1.36	0.058	0.009	0.085	0.035	0.084	0.025	0.208	0.019	1.97	0.23	3.16	1.16
buried (Unit I)	9	8.41	3.39	13.74	4.35	3.35	1.06	5.63	2.35	0.056	0.015	0.085	0.036	0.062	0.031	0.095	0.002	1.86	0.48	2.39	1.02
buried (Unit II)	6	7.45	1.13	8.96	5.81	2.69	0.25	2.97	2.35	0.083	0.020	0.122	0.068	0.042	0.015	0.062	0.017	1.52	0.17	1.67	1.28
sea-bed (inside)	6	9.90	0.94	10.78	8.47	3.43	0.45	4.09	2.85	0.062	0.010	0.075	0.053	0.061	0.011	0.075	0.044	1.52	0.27	1.90	1.32
hydrothermal	1	1.11	-	1.11	1.11	0.67	-	0.67	0.67	0.039	-	0.039	0.039	0.029	-	0.029	0.029	0.91	-	0.91	0.91

		Mg				Na				K				Mn/Fe				Cu+Ni+Zn			
total	169	1.33	0.25	2.14	0.97	1.70	0.19	2.70	1.21	0.87	0.30	2.13	0.44	1.20	1.11	14.97	0.35	0.71	0.23	1.57	0.25
sea-bed(bulk)	147	1.30	0.23	1.95	0.97	1.71	0.16	2.61	1.42	0.83	0.28	1.84	0.44	1.11	0.24	2.46	0.57	0.71	0.22	1.40	0.25
buried (Unit I)	9	1.48	0.37	2.12	1.13	1.83	0.37	2.70	1.47	1.08	0.50	2.13	0.60	1.31	0.95	3.72	0.35	0.76	0.36	1.57	0.43
buried (Unit II)	6	1.71	0.25	2.14	1.43	1.56	0.07	1.67	1.47	1.14	0.15	1.43	1.02	1.08	0.14	1.34	0.93	0.83	0.32	1.40	0.52
sea-bed (inside)	6	1.31	0.13	1.50	1.12	1.44	0.15	1.63	1.30	1.11	0.16	1.33	0.94	1.11	0.38	1.85	0.86	0.69	0.20	0.95	0.47
hydrothermal	1	1.87	-	1.87	1.87	1.21	-	1.21	1.21	1.26	-	1.26	1.26	14.97	-	14.97	14.97	0.37	-	0.37	0.37

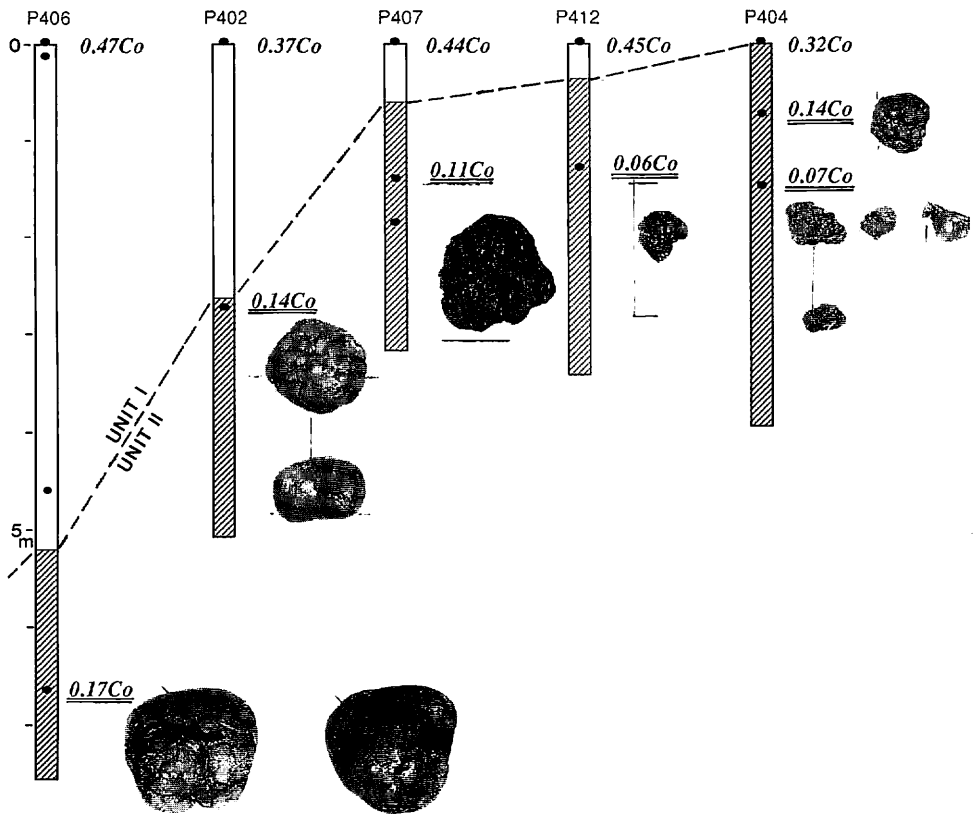

Fig. IX-6 Nodules buried in Unit II and their Co concentration (wt. %) in comparison with sea-bed nodules. Note significant depletion of Co.

Bulk chemical analysis shows marked difference in Co concentration and smectite content. Though the Co concentrations of sea-bed nodules and Unit I nodules are within the same range (0.3-0.5% Co), the Unit II nodules are significantly depleted in Co ranging from 0.06 to 0.17%. Furthermore the Unit II nodules are rich in smectite but phillipsite is not detected (Table IX-3 and Fig. IX-6).

The buried nodules are considered to be dropped off from uplifting, and kept buried in the sediments while most nodules have been continuously uplifted during their growth. Is it possible to correlate buried older nodules and uplifted sea-bed

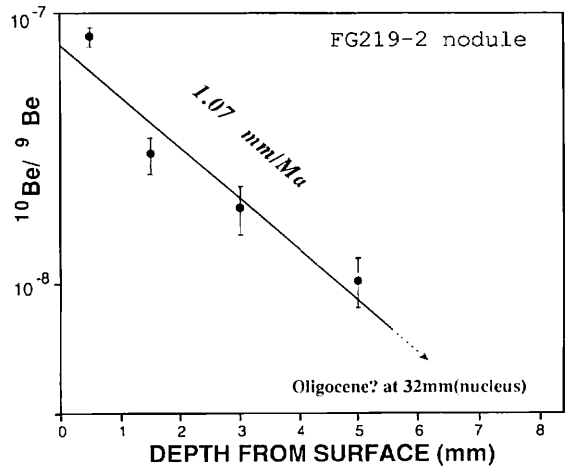

Fig. IX-7 Growth rate of a manganese nodule collected within this area during the cruise GH80-1 (13°47.15S, 159°28.26'W; 5147 m water depth). Analyzed by Dr. Teruo Inoue at Daiich Isotope Laboratory.

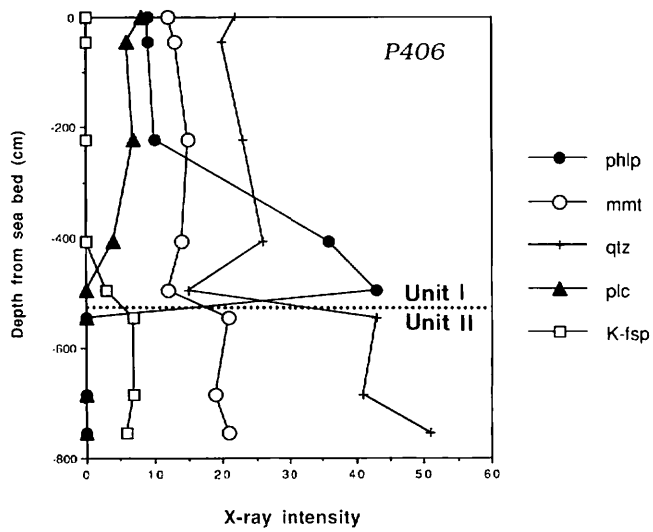

Fig. IX-8 Downcore change in mineral composition of core sediments from P406.

nodules on the modern sea floor? As growth rate of deep-sea nodules is in the order of mm/m.y., the larger nodules should have longer growth history. In fact, larger nodules have more complicated internal structure than smaller nodules even in a single site. Figures IX-2 and IX-5 for example show a textural variation from surface to nucleus. We found a common stratigraphic change in internal textural pattern within large nodules. Most of large nodules from various stations in the survey area include soft, porous old nodules (1-3 cm in diameter) at their center. Figure IX-5 demonstrates common stratigraphic variation of texture and a marked change in Co and smectite contents. The inner soft nodule are always depleted in Co (0.12-0.31%) and associated with abundant smectite. Also, the out surface of the soft nodule is surrounded by thin buserite layer as observed in microscope (Figure IX-2D and 2E).

The comparison reveals that small soft nodules had been formed during deposition of Unit II (Oligocene - Cretaceous) below long-term hiatus between Units I and II during which abundant growth of nodules may have taken place. A Be-10 dating shows a slow growth rate of 1.07 mm/m.y. (Figure IX-7) for a spherical nodule from an adjacent site. This suggests that the history of large nodules can go back to Oligocene or older, which agrees with the above interpretation.

Mineralogy of nuclei

The bulk mineral composition of 24 rock samples served as nuclei from 21 locations were examined by powder XRD analysis (Table IX-4). Most of nodule nuclei

Table IX-4 X-ray mineralogy of nodule nuclei.

No.	Sample no.	Qtz	Plc	Smt	Philp	others	rock name
3	FG659	2	-	6	-		claystone
4	FG614	2	-	5	-		claystone
6	FG708	1	-	5	-		claystone
1	FG680	3	-	4	-		claystone
2	FG676	5	-	4	-		claystone
5	FG692	4	-	4	-		claystone
7	FG631	-	-	4	-		claystone
8	FG691	3	-	4	-		claystone
11	FG619	2	-	4	-		claystone
18A	FG705	1	-	4	-		claystone
7A	FG631	2	tr	5	-		claystone
10	FG667	1	-	3	6		zeolitic claystone
21	FG704	-	-	2	10	Cptl	zeolitic claystone
12	FG668	1	-	1	10		zeolite stone
17	FG664	-	-	-	10		zeolite stone
9	P409/top	-	-	1	7		zeolite stone
16	FG625	-	-	1	4		zeolite stone
15	FG694	7	10	1	-		altered basalt
18	FG705	3	10	1	-		altered basalt
14	FG632	-	8	3	-		altered basalt
13	FG666	-	10	-	-	Cpx, Il?	altered basalt
13A	FG666	-	3	-	-	Cpx, Il?	altered basalt
20	FG585	10	-	-	-		chert
19	FG646	-	-	-	-	Ap	fossil

Note: Qtz=quartz, Pc=plagioclase, Sm=smectite, Ph=phillipsite
Cpx=clinopyroxene, Il=illite, Ap=apatite, Cptl=clinoptilolite

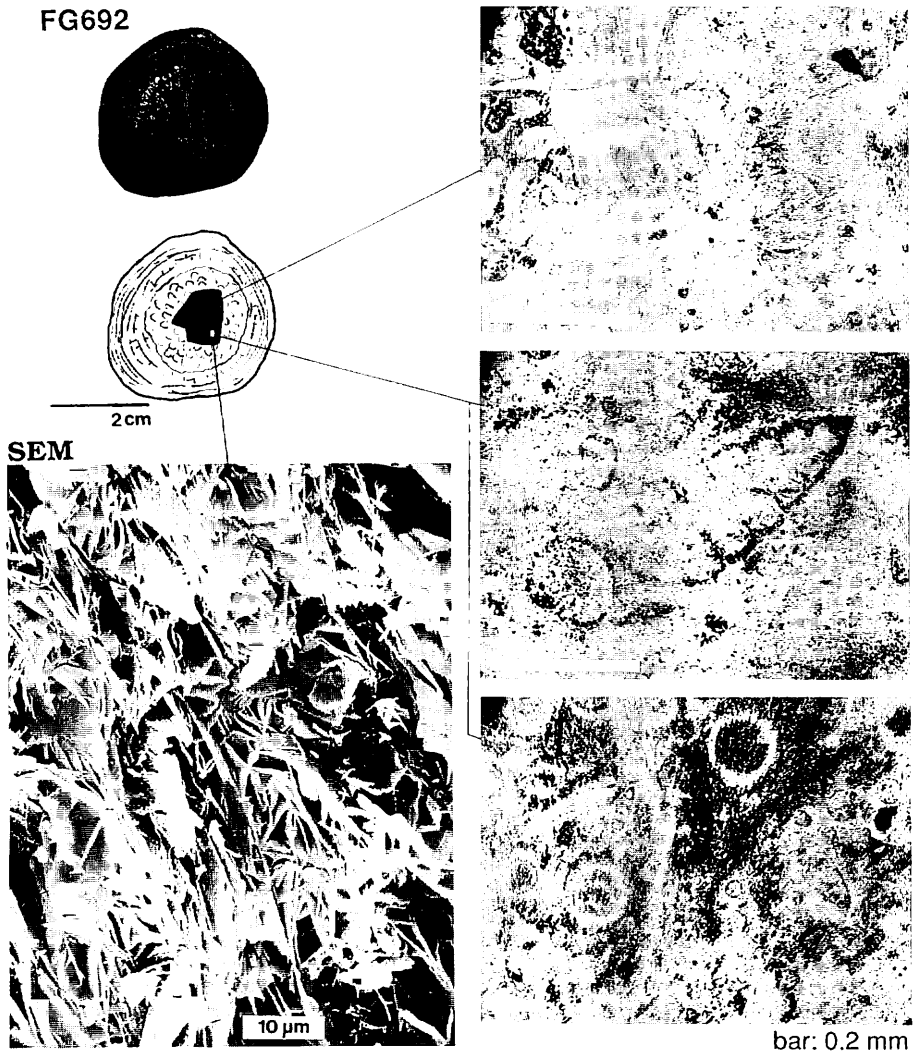

Fig. IX-9 Photomicrographs of hydrothermal manganese mineral (todorokite) in three nodules served as nuclei (FG692 and FG634) and developed as thin disconnected layer (FG693). SEM means scanning electron micrograph. Note large single crystals of todorokite.

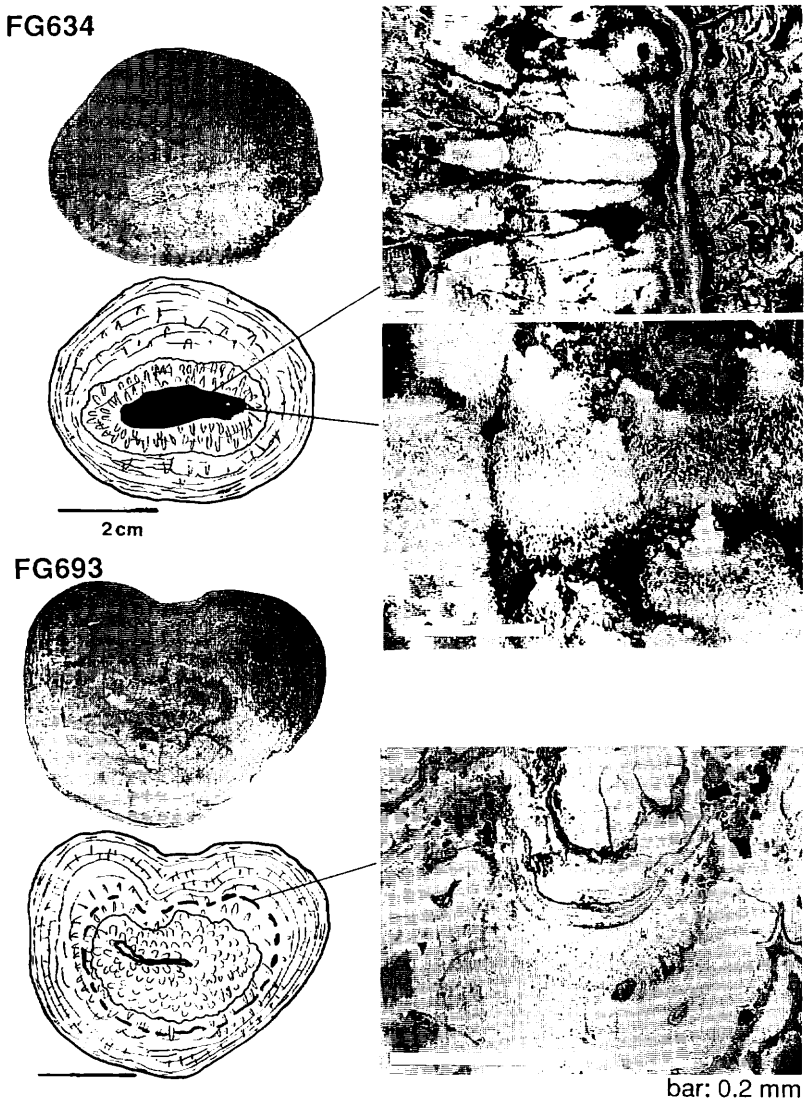

Fig. IX-9 (continued)

are composed of consolidated clayey stones with buff to brown color. The clayey stones are classified with mineral composition into the stiff pelagic clay (major smectite and minor quartz) and the zeolitic siltstone (phillipsite). Figure IX-8 shows a consistent variation of detrital minerals in cores with that within manganese nodules. The areal distribution of these two types of nuclei are well correlated with that of substrate lithology. Sea-bed nodules above Unit II include the stiff clay as nuclei, while nodules of crusts above Unit III include zeolitic siltstone. This relationship means the nuclei has been uplifted from then sea floor during nodule growth and slow sedimentation of Unit I.

Shark teeth (ranging less than 1 cm to about 8 cm across), highly weathered basaltic rocks, and fragments of chert occasionally are served as nuclei of nodules.

Hydrothermal manganese mineral within nodules

The FG692 and possibly FG693 nodules contain angular fragments of hydrothermal manganese deposits as nuclei. A nucleus of a FG692 nodule yields siliceous microfossils (*Dictyomitra*-type radiolarian) which is totally cemented by pure todorokite crystals (Figure IX-9). A similar hydrothermal manganese mineral is observed in FG693 nodule as disconnected thin layers on a polished section (Figure IX-9).

The chemical composition (the last row in Appendix IX-1) is clearly within the range of hydrothermal manganese deposits found from recent mid-oceanic ridges, backarc basins and submarine volcanos (Corliss *et al*, 1978; Lonsdale *et al*., 1980; Cronan *et al*., 1982; Usui *et al*., 1986). It is characterized by high Mn/Fe ratio, low transition elements except for Mn, and negligible amount of detrital minerals. The mineral is most probably a heat-resistant todorokite, because it retains as 10 Å mineral after heating at 110°C for 2 hours.

The age of radiolarian show that a low-temperature hydrothermal activity took place in Cretaceous or later, probably related to sea floor spreading which formed the Manihiki Plateau in 100-110 Ma or later (Jackson and Schlanger, 1976).

Summary

1) Nodules of this area are in principle composed of major vernadite with minor amounts of buserite developed in their interior, and detrital silicate minerals. The nodules have been growing since Paleogene time or older to form hydrogenetic ferromanganese mineral influenced by a slight diagenetic process of surface sediments in the past.

2) The nodules buried within subbottom Paleogene clay sediments (Unit II) are most likely correlated to the innermost old nodules within some large nodules on the sea bed in terms of texture, Co concentration, and accessory detrital minerals. In contrast, buried nodules in Unit I can be correlated to younger generation of sea bed nodules.

3) A rare but positive occurrence of hydrothermal manganese deposits as nodule nuclei suggest a low-temperature hydrothermal activity related to sea floor spreading to form the Manihiki Plateau during Cretaceous time or later.

References

Burns, R.G. and Burns, V.M. (1977) Mineralogy of Manganese Nodules. In: G.P. Glasby (ed.), *Marine Manganese Deposits,* Elsevier Pub. Co. Ltd., p. 185-248.

————, Burns, V.M. and Stockman, H.W. (1983) A review of the todorokite-buserite problem: implication to the mineralogy of marine manganese nodules. *Amer. Mineral.*, vol. 68, p. 972-980.

Corliss, J.B., Lyle, M., Dymond, J. and Crane, K. (1978) The geochemistry of hydrothermal mounds near the Galapagos rift. *Earth Planet. Sci.* Lett., vol. 40, p. 1224.

Cronan, D.S., Glasby, G.P., Moorby, S.A., Thomson, J., Knedler, K.E. and McDougall, J.C. (1982) A submarine hydrothermal manganese deposit from the S.W. Pacific Island Arc. *Nature*, vol. 298, p. 456-458.

Giovanoli, R. (1980) On natural and synthetic manganese nodules. In: Varentsov, I. (ed.), *Geology and Geochemistry of Manganese,* Hungarian Acad. Sci. Publ., vol. 1, p. 159-202.

Hein, J., Morgenson, L.A., Clague, D.A. and Koski, R.A. (1987) Cobalt-rich ferromanganese crusts from the exclusive Economic zone of the United States and nodules from the Oceanic Pacific. In: D.W. Scholl and J.G. Vedder (eds.), *Geology and Resource Potential of the Continental Margin of Western North America and Adjacent Ocean Basins-Beaufort Sea to Baja California,* CPCEMR, Houston, p. 753-771.

Jackson, E.D. and Schlanger, S.O. (1976) Regional synthesis, Line Islands chain, Tuamotu Island chain, and Manihiki Plateau, Central Pacific Ocean. In: *DSDP Initial Rept.*, N.S.F., vol. 33, p. 915-927.

Lonsdale, P., Burns, V.M. and Fisk, M. (1980) Nodules of hydrothermal birnessite in the caldera of a young seamount. *J. Geol.*, vol. 88, p. 611-618.

Mochizuki, T. and Terashima, S. (1983) Chemical analysis of manganese nodules. *Methods of Chemical Analysis in G.S.J.*, no. 53, p. 1-36.

Ostwald, J. (1984) Ferruginous vernadite in an Indian Ocean ferromanganese nodule. *Geol. Mag.*, vol. 121, no. 5, p. 483-488.

Stouff, P. and Boulègue, J. (1988) Synthetic 10-Å and 7-Å phyllomanganates; their structures as determined by EXAFS. *Amer. Mineral.*, vol. 73. p. 1162-1169.

Terashima, S. (1978) Atomic absorption analysis of Mn, Fe, Cu, Ni, Co, Pb, Zn, Si, Al, Ca, Mg, Na, K, Ti, and Sr in manganese nodules. *Bull. Geol. Surv. Japan*, vol. 29, p. 401-411.

Usui, A. (1979a) Minerals, metal contents, and mechanism of formation of manganese nodules from the Central Pacific Basin (GH76-1 and GH77-1 areas). In: Bischoff, J.L. and Piper, D.Z. (eds.), *Marine Geology and Oceanography of the Pacific Manganese Nodule Provinces,* Plenum Pub. Co., p. 651-679.

————, Yuasa, M., Yokota, M., Nishimura, A. and Murakami, F. (1986) Submarine hydrothermal manganese deposits from the Ogasawara (Bonin) Arc, off the Japan Islands. *Mar. Geol.*, vol. 73, p. 311-322.

————, Mellin, T.A., Nohara, M. and Yuasa, M. (1989) Structural stability of marine 10 Å manganates from the Ogasawara (Bonin) Arc: Implication for low-temperature hydrothermal activity. *Mar. Geol.*, vol. 86, p.41-56.

Appendix IX-1 Chemical and mineral composition of manganese nodules.

#	st#	Sam#	horizon	shape	size (cm)	n	part	depth	Mineralogy						Chemistry													
									bus.	ver.	qz	ph	pc	sm	Mn	Fe	Cu	Ni	Co	Si	Al	Zn	Pb	Ca	Mg	Na	K	H+	H-
1	3913	FG587	top	ID	2	1	whole		27	11	7	5	4	0	22.06	12.24	0.524	0.798	0.321	6.08	3.12	0.081	0.076	2.70	1.90	1.73	0.70	10.60	19.92
2	3915	FG589	top	S	1.5	1	1/2		16	13	14	4	0	0	20.51	14.42	0.345	0.621	0.409	6.42	3.05	0.067	0.111	2.03	1.54	1.75	0.69	10.87	20.96
3	3917	FG591	top	ID	2.5	1	1/2		12	14	12	0	0	0	21.02	14.72	0.342	0.644	0.422	6.22	2.84	0.064	0.102	1.97	1.56	1.74	0.71	10.20	21.60
4	3918	FG592	top	IS	1	3	whole		21	12	12	21	0	0	19.20	12.50	0.399	0.779	0.310	8.29	3.84	0.071	0.087	1.80	1.81	2.02	1.25	10.04	18.01
5	3927	FG606S	top	IS	1-1.5	2	whole		11	10	5	20	0	0	17.30	14.13	0.326	0.504	0.347	8.62	3.72	0.057	0.092	1.81	1.51	1.87	1.11	10.57	19.28
6		FG606T1	top	T	12	1	top	0-1mm	0	7	5	7	0	0	13.44	22.25	0.069	0.145	0.529	7.22	2.00	0.036	0.133	1.90	1.00	1.81	0.68	11.14	17.45
7		FG606T2	top	T	12	1	bottom	0-2mm	5	12	14	32	5	0	12.08	10.60	0.221	0.369	0.198	13.68	5.12	0.035	0.068	1.47	1.42	2.24	1.76	9.90	17.65
8		FG606T3	top	T	12	1	inside	2-10mm	7	11	7	0	0	0	19.71	19.18	0.160	0.337	0.501	4.78	1.81	0.044	0.118	1.93	1.07	1.82	0.53	11.87	20.54
9		FG606T	top	T	3	1	whole		14	9	0	4	4	0	17.91	19.93	0.251	0.441	0.399	5.47	2.30	0.056	0.124	1.80	1.28	1.49	0.56	10.90	20.71
10	3930	FG609M	top	ID	2	1	whole		12	14	9	12	5	0	15.94	14.80	0.267	0.456	0.305	8.09	3.59	0.050	0.082	1.74	1.33	1.69	1.01	10.55	19.74
11		FG609T	top	T	6	1	bottom	0-10mm	4	12	7	9	0	0	14.73	18.29	0.227	0.344	0.301	8.02	3.60	0.058	0.086	1.69	1.20	1.68	0.86	9.33	20.62
12		FG609S	top	IDP	1-2	2	whole		16	9	4	18	4	0	15.45	12.61	0.330	0.539	0.271	11.71	4.42	0.054	0.061	1.70	1.48	2.09	1.55	9.78	17.30
13	3953	FG633	top	S	2.2	1	1/2		14	12	9	7	0	0	19.92	15.19	0.295	0.589	0.427	6.85	2.93	0.063	0.096	1.92	1.43	1.64	0.75	9.97	22.08
14	3954	FG634	top	IS	3	1	1/4		5	15	12	5	0	0	18.11	17.87	0.164	0.353	0.504	7.22	2.72	0.048	0.109	1.99	1.10	1.64	0.74	9.51	22.64
15	3955	FG635S	top	S	3	1	1/4		0	16	7	0	0	0	18.82	18.05	0.160	0.358	0.517	6.32	2.44	0.050	0.114	2.01	1.08	1.56	0.65	9.56	23.82
16		FG635M	top	ID	1.5	2	whole		4	11	7	21	0	0	15.26	14.39	0.204	0.352	0.376	9.74	3.73	0.045	0.101	1.78	1.11	1.94	1.32	9.74	20.14
17	3956	FG636	top	S	2	1	1/2		4	15	13	0	0	0	17.48	17.77	0.175	0.356	0.458	6.60	2.62	0.049	0.105	1.92	1.11	1.58	0.63	10.24	22.85
18	3957	FG637L	top	S	3.5	1	1/8		0	14	12	4	0	0	17.66	18.52	0.131	0.296	0.545	6.68	2.43	0.045	0.120	2.09	0.99	1.65	0.64	9.86	24.44
19		FG637M	top	S	2.5	1	1/4		0	14	10	0	0	0	16.31	18.26	0.145	0.296	0.489	6.43	2.38	0.045	0.105	1.89	1.01	1.57	0.60	9.68	24.00
20		FG637S	top	ID	1	4	whole		4	13	9	12	0	0	16.51	15.39	0.210	0.372	0.398	7.76	3.37	0.048	0.074	1.95	1.13	1.83	0.97	9.19	22.94
21	3958	FG638	top	IS	2	1	1/2		4	11	4	9	0	0	16.51	15.66	0.211	0.379	0.421	8.81	3.44	0.046	0.104	1.97	1.16	1.82	0.99	9.09	23.68
22	3959	FG639	top	IS	2	1	1/2		0	16	5	0	0	0	16.15	19.63	0.149	0.315	0.524	6.35	2.41	0.047	0.125	1.97	1.07	1.55	0.58	9.89	24.05
23	3960	FG640L1	top	S	4	1	surface	0-10mm	4	19	4	5	5	0	17.96	17.97	0.159	0.372	0.620	5.77	2.10	0.048	0.122	2.21	1.06	1.59	0.61	9.88	24.37
24		FG640L2	top	S	4	1	inside, soft	10-20mm	12	18	21	0	4	0	15.87	17.14	0.223	0.657	0.126	9.01	3.08	0.073	0.067	1.37	1.50	1.30	1.07	8.74	19.20
25		FG640M	top	IS	2	1	whole		4	11	5	0	0	0	16.23	18.29	0.168	0.410	0.503	6.32	2.40	0.054	0.108	2.00	1.16	1.51	0.61	10.05	22.49
26		FG640S	top	IS	1	3	whole		7	12	7	11	0	0	17.46	15.84	0.227	0.432	0.426	7.39	3.12	0.053	0.099	1.90	1.19	1.67	0.96	10.41	20.20
27	3961	FG641	top	S	2	1	whole		4	13	8	7	0	0	16.61	15.83	0.159	0.373	0.411	6.64	2.50	0.044	0.085	1.86	1.00	1.42	0.59	10.33	22.05
28	3964	FG644L1	top	S	4	1	surface	0-12mm	4	15	14	4	0	0	20.22	16.54	0.158	0.442	0.549	5.64	2.21	0.048	0.093	2.10	1.11	1.58	0.62	10.23	22.78
29		FG644L2	top	S	4	1	inside, soft	12-20mm	9	19	44	0	0	9	16.60	14.43	0.172	0.547	0.178	10.25	3.28	0.060	0.064	1.32	1.35	1.33	1.12	10.03	19.68
30		FG644S	top	ID	0.5-1	9	whole		16	9	5	18	0	0	16.97	12.81	0.275	0.571	0.321	9.29	3.71	0.059	0.070	1.51	1.37	1.84	1.26	7.50	18.41

Appendix IX-1 (continued)

#	st#	Sam#	horizon	shape	size n (cm)	part	depth	Mineralogy bus.	ver.	qz	ph	pc	sm	Chemistry Mn	Fe	Cu	Ni	Co	Si	Al	Zn	Pb	Ca	Mg	Na	K	H+	H-
31	3965	FG645L	top	ID	1	3 whole		20	10	0	23	0	0	18.95	12.07	0.327	0.721	0.314	8.89	3.64	0.071	0.063	1.79	1.74	1.91	1.38	8.77	17.78
32		FG645S	top	IS	0.5	6 whole		20	8	7	25	0	0	17.26	12.88	0.340	0.669	0.297	9.39	4.00	0.069	0.067	1.60	1.72	1.87	1.42	9.53	16.77
33	3966	FG646	top	S	0.5-1	6 whole		25	9	5	27	0	0	17.53	12.14	0.334	0.689	0.275	10.26	3.92	0.066	0.062	1.62	1.69	1.89	1.41	9.83	16.68
34	3968	FG648	top	IS	1-1.5	3 whole		30	10	7	16	0	0	20.35	11.66	0.393	0.814	0.284	7.91	3.45	0.079	0.074	1.75	1.86	1.81	1.03	9.75	18.75
35	3969	FG649	top	IS	2.5	1 1/2		5	15	0	0	0	0	16.86	19.22	0.144	0.321	0.503	6.61	2.46	0.051	0.106	1.98	1.14	1.59	0.59	9.55	23.60
36	3971	FG651	top	IS	3	1 1/2		9	12	21	5	0	0	18.18	15.95	0.230	0.428	0.465	8.23	2.96	0.058	0.091	2.26	1.26	1.64	0.87	9.01	22.21
37	3972	FG652	top	IS	2	1 whole		4	14	5	0	0	0	17.40	18.93	0.186	0.350	0.492	6.87	2.54	0.053	0.106	1.95	1.18	1.51	0.66	9.69	23.22
38	3973	FG653M	top	IS	2	1 whole		16	13	18	0	0	4	19.55	14.42	0.363	0.691	0.410	7.42	3.26	0.074	0.073	1.88	1.72	1.65	0.82	10.26	21.47
39		FG653T1	top	T	8	1 top	0-2mm	0	12	0	0	0	0	14.89	23.98	0.097	0.171	0.455	6.09	1.59	0.046	0.146	1.98	1.00	1.64	0.47	7.29	24.00
40		FG653T2	top	T	8	1 bottom	0-3mm	27	11	5	28	0	0	18.03	7.32	0.584	0.721	0.200	11.32	4.79	0.070	0.050	1.69	1.59	2.61	1.70	9.92	17.47
41		FG653T3	top	T	8	1 inside	2-10mm	4	10	9	5	4	0	17.03	17.02	0.247	0.385	0.352	7.89	2.75	0.054	0.095	2.04	1.25	1.96	0.83	9.41	19.80
42	3974	FG654L1	top	S	6	1 surface	0-2mm	5	10	0	0	0	0	15.19	22.13	0.163	0.200	0.541	6.35	2.06	0.047	0.134	1.89	1.05	1.49	0.52	9.41	23.83
43		FG654L2	top	S	6	1 inside	2-14mm	4	17	16	0	0	0	19.70	17.83	0.169	0.356	0.602	5.60	2.26	0.052	0.123	2.14	1.13	1.70	0.69	8.99	24.90
44		FG654L3	top	S	6	1 inside, soft	14-30mm	4	19	34	0	9	9	14.92	16.80	0.167	0.364	0.130	10.78	3.67	0.059	0.075	1.37	1.38	1.45	1.33	8.03	25.65
45		FG654M1	top	S	3	1 surface	0-1mm	0	12	4	0	0	0	13.24	23.32	0.091	0.132	0.518	6.58	2.06	0.044	0.131	1.80	1.00	1.45	0.44	10.63	24.35
46		FG654M2	top	S	3	1 inside	1-12mm	7	13	5	5	0	0	17.19	17.67	0.188	0.367	0.513	6.46	2.66	0.054	0.115	1.94	1.12	1.64	0.78	10.86	21.45
47		FG654S	top	ID	1	3 whole		4	17	25	16	0	0	16.29	15.00	0.261	0.397	0.412	9.70	4.01	0.059	0.104	1.93	1.25	1.98	1.42	7.16	23.34
48	3976	FG655L	top	S	4	1 1/2		0	18	12	0	0	0	17.99	17.06	0.167	0.383	0.469	7.41	3.04	0.054	0.088	2.15	1.18	1.71	0.73	7.21	25.84
49		FG655S	top	IS	1-1.5	3 whole		18	10	7	16	0	0	19.15	14.06	0.325	0.592	0.357	7.48	3.41	0.068	0.090	2.13	1.58	1.85	1.02	8.59	21.90
50	3980	FG659L1	top	IS	6	1 surface	0-0.5mm	0	15	0	0	0	0	19.18	19.33	0.149	0.308	0.615	5.71	1.87	0.055	0.121	2.27	1.10	1.70	0.65	7.30	26.68
51		FG659L2	top	IS	6	1 inside	0.5-7mm	0	16	0	0	0	0	20.64	19.08	0.131	0.300	0.523	3.69	1.36	0.054	0.160	2.59	0.97	1.64	0.54	9.43	26.22
52		FG659L3	top	IS	6	1 inside, soft	7-25mm	0	20	34	5	0	0	15.32	15.95	0.127	0.318	0.313	10.24	3.58	0.053	0.066	1.90	1.12	1.63	0.94	9.28	22.13
53		FG659M	top	S	2	1 whole		0	16	0	0	0	0	18.40	18.50	0.140	0.310	0.465	5.88	2.27	0.048	0.088	2.20	1.02	1.66	0.71	4.93	25.19
54		FG659S	top	S	1	4 whole		0	12	9	9	0	0	17.85	14.17	0.226	0.427	0.309	8.06	3.11	0.053	0.057	2.14	1.13	1.84	1.03	10.07	22.93
55		FG659T	top	T	2	1 whole		0	12	0	0	0	0	17.95	17.85	0.207	0.321	0.406	5.87	2.38	0.055	0.096	2.08	1.09	1.59	0.58	10.37	23.14
56	3983	FG662	top	IS	1	2 whole		18	5	5	34	0	0	15.97	12.93	0.280	0.571	0.286	9.62	3.77	0.060	0.071	1.62	1.48	1.91	1.47	10.30	17.03
57	3985	FG664	top	IS	2	1 whole		11	11	0	20	0	0	16.23	15.35	0.210	0.421	0.384	8.86	3.56	0.059	0.055	1.77	1.25	1.99	1.36	8.02	21.53
58	3986	FG665L	top	ID	6	1 1/8		0	21	27	7	0	0	17.75	15.87	0.177	0.374	0.443	7.47	2.73	0.051	0.060	2.06	1.12	1.75	0.81	9.23	22.79
59		FG665M	top	IS	2	1 1/2		5	20	14	0	0	0	17.77	18.10	0.204	0.372	0.416	7.04	2.80	0.056	0.106	1.60	1.21	1.51	0.87	8.23	14.70
60		FG665S	top	ID	0.5-1.5	3 whole		7	13	7	0	0	4	15.45	14.27	0.278	0.430	0.335	9.68	4.04	0.060	0.057	1.75	1.46	1.81	1.42	7.68	19.69

Appendix IX-1 (continued)

#	st#	Sam#	horizon	shape	size (cm)	n	part	depth	Mineralogy bus.	ver.	qz	ph	pc	sm	Chemistry Mn	Fe	Cu	Ni	Co	Si	Al	Zn	Pb	Ca	Mg	Na	K	H+	H-
61	3987	FG666	top	IDP	2	1	whole		14	11	0	12	0	0	15.60	16.22	0.262	0.504	0.327	7.94	3.32	0.062	0.062	1.71	1.56	1.63	1.00	8.86	21.45
62	3988	FG667	top	ID	2	1	whole		16	13	7	23	0	0	13.56	11.52	0.288	0.535	0.237	10.44	4.38	0.060	0.043	1.54	1.43	2.16	1.84	9.66	16.43
63	3989	FG668	top	S	2	1	whole		0	14	9	0	0	0	17.13	17.35	0.169	0.362	0.488	5.68	2.38	0.056	0.092	1.92	1.11	1.54	0.62	10.87	21.53
64	3992	FG671	top	IS	2	1	1/4		9	16	19	3	0	0	17.08	14.51	0.254	0.538	0.360	6.92	2.79	0.065	0.063	1.79	1.39	1.63	0.89	8.05	22.47
65	3994	FG673	top	T	9	1	bottom	0-10mm	4	11	15	18	0	0	14.69	14.83	0.196	0.329	0.359	9.02	3.16	0.047	0.057	1.96	1.04	1.98	1.21	11.97	21.23
66	3996	FG675	top	S	2	1	1/2		4	14	10	4	0	0	16.63	17.48	0.175	0.352	0.495	6.50	2.74	0.054	0.088	1.98	1.13	1.62	0.68	8.03	23.56
67	3997	FG676	top	T	4	1	1/3		12	10	12	18	0	3	17.09	14.57	0.292	0.464	0.403	7.73	3.10	0.060	0.072	1.93	1.30	1.77	1.01	9.73	22.63
68	3998	FG677	top	IS	1.5	1	whole		4	12	9	4	0	0	17.06	17.31	0.198	0.426	0.477	6.05	2.66	0.062	0.091	1.90	1.21	1.61	0.70	10.34	22.08
69	3999	FG678	top	IS	3	1	1/4		4	12	10	4	0	0	16.43	18.02	0.165	0.364	0.463	6.22	2.56	0.054	0.085	1.89	1.06	1.61	0.67	10.02	22.45
70	4000	FG679L	top	S	3	1	1/4		0	13	10	0	0	0	16.60	17.98	0.165	0.331	0.492	6.16	2.48	0.051	0.072	2.08	1.07	1.61	0.70	9.44	23.81
71		FG679S	top	IDP	1-1.5	2	whole		9	13	4	0	0	0	17.75	13.69	0.293	0.460	0.339	6.82	3.06	0.061	0.068	2.07	1.27	1.53	0.70	10.11	21.47
72	4001	FG680L	top	ID	6	1	1/8		4	11	10	12	0	0	16.77	15.74	0.148	0.334	0.426	7.40	2.61	0.054	0.079	2.00	1.04	1.74	0.86	10.05	22.35
73		FG680M	top	S	2.5	1	1/4		4	11	12	6	0	0	18.29	17.14	0.200	0.372	0.440	6.80	2.67	0.058	0.080	1.98	1.15	1.64	0.70	8.92	23.45
74		FG680S	top	ID	1	4	whole		13	13	6	10	0	0	19.43	13.27	0.375	0.527	0.408	7.54	3.62	0.067	0.059	1.88	1.50	1.71	0.92	9.06	21.88
75	4002	FG681L1	top	S	7	1	surface	0-1mm	0	12	0	0	0	0	17.46	19.67	0.132	0.234	0.524	5.88	1.93	0.050	0.111	2.11	1.03	1.59	0.59	9.16	23.99
76		FG681L2	top	S	7	1	inside	1-10mm	0	16	0	9	0	0	19.26	17.26	0.116	0.276	0.623	5.50	2.10	0.046	0.099	2.24	0.97	1.77	0.74	9.52	24.24
77		FG681L3	top	S	7	1	inside	10-12mm	0	16	16	7	0	0	20.81	14.50	0.110	0.378	0.622	6.27	2.41	0.044	0.060	2.49	1.02	1.83	0.72	9.18	25.45
78		FG681L4	top	S	7	1	inside	12-20mm	0	15	43	0	0	0	18.47	13.67	0.119	0.401	0.501	9.42	3.26	0.056	0.075	2.59	1.04	1.88	0.95	6.75	24.35
79		FG681L5	top	S	7	1	inside, soft	20-22mm	3	15	44	0	0	6	20.96	11.33	0.166	0.623	0.346	8.47	2.85	0.075	0.052	1.83	1.30	1.61	0.95	8.91	22.49
80		FG681L6	top	S	7	1	inside, soft	22-32mm	0	19	31	0	0	9	13.97	16.25	0.116	0.297	0.120	10.64	4.09	0.053	0.044	1.35	1.20	1.33	1.24	9.09	18.95
81		FG681T	top	T	2	1	whole		0	13	3	0	0	0	15.63	19.04	0.120	0.230	0.454	5.57	2.13	0.051	0.098	1.89	1.11	1.53	0.47	8.57	23.55
82		FG681M1	top	IS	4	1	surface	0-1mm	0	10	0	0	0	0	14.99	18.95	0.107	0.208	0.471	5.54	1.89	0.046	0.093	1.84	1.05	1.42	0.46	7.02	26.79
83		FG681M2	top	IS	4	1	inside	1-15mm	0	15	12	0	0	0	17.87	16.37	0.159	0.334	0.474	6.13	2.68	0.052	0.085	2.03	1.15	1.74	0.64	7.82	24.46
84		FG681S	top	IDP	1-1.5	2	whole		6	10	9	6	0	0	15.72	13.75	0.192	0.355	0.366	5.87	2.74	0.051	0.047	1.85	1.14	1.55	0.65	8.00	23.00
85	4003	FG682	top	S	2	1	1/4		0	12	10	0	0	0	17.21	17.55	0.138	0.294	0.471	6.34	2.56	0.052	0.077	2.02	1.15	1.64	0.60	10.06	23.36
86	4004	FG683	top	ISP	1.5	1	1/2		6	14	10	7	0	0	17.60	15.72	0.213	0.430	0.457	6.58	2.85	0.062	0.059	1.96	1.36	1.65	0.69	9.79	21.95
87	4005	FG684	top	D	4	1	whole		10	12	7	7	0	0	19.03	14.19	0.288	0.546	0.422	6.66	3.04	0.069	0.078	1.86	1.51	1.74	0.90	8.15	22.66
88	4006	FG685	top	ID	4	1	1/2		22	9	7	4	0	0	20.16	14.40	0.398	0.688	0.360	6.82	3.02	0.079	0.064	2.13	1.86	1.68	0.73	7.70	21.41
89	4007	FG686L	top	S	4	1	whole		3	14	15	16	0	0	17.72	15.18	0.163	0.393	0.462	7.65	2.84	0.055	0.055	2.18	1.21	1.73	0.73	9.12	23.15
90		FG686M	top	S	2	1	whole		6	14	9	6	0	0	18.06	15.23	0.199	0.408	0.439	6.36	2.93	0.057	0.083	2.05	1.31	1.69	0.70	9.90	23.01

Appendix IX-1 (continued)

#	st#	Sam#	horizon	shape	size (cm)	n	part	depth	Mineralogy						Chemistry													
									bus.	ver.	qz	ph	pc	sm	Mn	Fe	Cu	Ni	Co	Si	Al	Zn	Pb	Ca	Mg	Na	K	H+	H-
91		FG686S	top	IS	1	4	whole		12	11	9	13	0	0	17.97	13.99	0.264	0.503	0.405	7.40	3.31	0.065	0.058	1.98	1.56	1.82	0.84	6.19	23.53
92	4008	FG687	top	S	2.5	1	1/4		3	12	6	0	0	0	18.05	15.73	0.162	0.373	0.475	5.78	2.45	0.056	0.068	1.98	1.22	1.59	0.62	8.57	23.32
93	4009	FG688L	top	S	3	1	1/8		4	12	19	15	0	0	18.43	15.20	0.141	0.350	0.499	6.73	2.49	0.055	0.069	2.09	1.19	1.67	0.73	7.93	23.42
94		FG688M	top	S	2	1	1/2		4	13	6	7	0	0	18.11	17.79	0.187	0.400	0.461	5.68	2.65	0.062	0.087	1.97	1.28	1.56	0.66	9.02	21.42
95		FG688S	top	IS	1-1.5	1	whole		6	14	9	0	0	0	18.60	16.79	0.209	0.464	0.445	6.27	2.84	0.068	0.068	1.96	1.38	1.63	0.71	6.44	23.33
96		FG688vS	top	IS	1	3	whole		9	13	6	15	0	0	16.11	12.98	0.251	0.447	0.345	8.01	3.71	0.061	0.066	1.71	1.39	1.78	1.12	9.62	19.40
97	4010	FG689L	top	IS	6	1	1/8		0	12	15	0	0	0	18.45	16.27	0.174	0.378	0.512	6.73	2.53	0.055	0.085	2.06	1.20	1.75	0.76	8.37	23.18
98		FG689M	top	S	3.5	1	1/8		9	11	15	0	0	0	18.35	15.88	0.165	0.420	0.470	6.49	2.72	0.060	0.072	2.06	1.29	1.65	0.76	8.86	23.14
99		FG689S	top	ID	1	4	whole		9	10	4	6	0	0	16.57	17.43	0.239	0.464	0.409	6.76	3.33	0.069	0.084	1.72	1.47	1.58	0.77	7.99	20.53
100	4011	FG690L	top	S	4	1	1/8		0	15	13	13	0	0	18.59	16.67	0.129	0.362	0.520	6.21	2.59	0.053	0.085	2.14	1.17	1.73	0.74	8.75	24.23
101		FG690M	top	S	2	1	whole		6	12	7	4	0	0	18.69	17.09	0.185	0.409	0.479	6.12	2.71	0.059	0.084	2.00	1.29	1.69	0.66	7.86	24.19
102		FG690S	top	ID	1	3	whole		9	10	7	9	0	0	17.43	15.32	0.252	0.440	0.442	7.19	3.16	0.063	0.068	1.97	1.40	1.80	0.88	8.92	21.73
103	4012	FG691L	top	S	4.5	1	whole		3	12	10	7	0	0	17.63	17.35	0.134	0.342	0.510	6.22	2.49	0.055	0.084	2.08	1.18	1.65	0.76	9.34	22.99
104		FG691M	top	S	2	1	1/2		4	12	7	0	0	0	17.41	17.81	0.156	0.357	0.499	5.72	2.43	0.057	0.090	1.99	1.18	1.58	0.64	9.40	23.23
105		FG691S	top	S	1	2	whole		10	8	7	7	0	0	17.34	16.67	0.246	0.425	0.443	6.37	2.95	0.063	0.079	1.90	1.42	1.65	0.71	8.26	22.32
106	4014	FG693	top	S	2	1	1/2		12	13	18	0	0	0	18.96	14.36	0.251	0.607	0.384	6.97	2.71	0.071	0.071	1.90	1.59	1.64	0.75	12.87	21.96
107	4015	FG694	top	X	1	3	whole		0	10	0	7	0	0	14.85	18.56	0.128	0.313	0.441	7.48	2.66	0.052	0.063	1.99	1.22	1.80	0.89	8.31	22.76
108	4016	FG695	top	X	3	1	whole	0-6mm	0	10	3	0	0	0	16.40	21.33	0.120	0.198	0.373	4.57	1.45	0.051	0.096	2.10	1.01	1.49	0.49	9.32	23.90
109	4019	FG698	top	ID	1-1.5	2	whole		13	11	4	18	0	0	15.34	13.23	0.267	0.563	0.290	8.85	3.73	0.063	0.066	1.72	1.61	1.95	1.41	9.48	17.96
110	4024	FG703L	top	S	4	1	1/2		0	14	10	6	0	0	16.35	17.59	0.147	0.321	0.477	6.09	2.49	0.052	0.085	2.01	1.15	1.64	0.70	10.04	23.27
111		FG703M	top	IS	2	1	whole		6	12	6	0	0	0	15.95	17.65	0.182	0.362	0.427	6.14	2.75	0.058	0.114	2.04	1.25	1.60	0.61	9.16	23.01
112		FG703S	top	IS	1	2	whole		9	13	4	9	0	0	15.32	13.67	0.227	0.395	0.376	7.43	3.41	0.054	0.057	1.94	1.30	1.75	0.95	10.72	20.80
113	4026	FG705L	top	IS	4	1	1/8		4	17	16	9	0	0	19.42	15.36	0.218	0.445	0.474	6.10	2.64	0.060	0.085	2.05	1.35	1.68	0.74	8.92	23.43
114		FG705M	top	IS	2	1	whole		4	15	10	3	0	0	18.14	17.03	0.189	0.397	0.444	5.99	2.76	0.060	0.062	1.95	1.28	1.63	0.65	9.27	22.72
115		FG705S	top	IS	1	4	whole		10	11	6	21	0	0	16.68	14.55	0.255	0.397	0.380	8.80	3.76	0.050	0.019	1.16	1.22	1.83	1.01	9.78	20.44
116	3934	FG613	top	IS	1-2	2	whole		16	10	3	21	0	0	17.20	11.96	0.306	0.642	0.282	9.36	3.83	0.070	0.048	1.84	1.65	2.08	1.55	8.92	18.75
117	3935	FG614	top	S	1.5	1	whole		22	12	6	3	0	0	21.02	12.42	0.372	0.782	0.330	6.33	3.23	0.085	0.050	2.05	1.95	1.74	0.79	8.41	22.08
118	3936	FG615	top	ID	3	1	1/2		15	9	9	10	0	0	19.22	14.16	0.287	0.562	0.373	6.22	2.91	0.067	0.062	2.17	1.49	1.79	0.80	10.19	22.27
119	3937	FG616	top	S	3	1	1/4		4	12	12	12	0	0	17.25	16.48	0.188	0.399	0.410	7.60	3.09	0.058	0.067	1.96	1.34	1.68	0.80	8.89	22.72
120	3938	FG617	top	S	2	1	whole		7	12	15	3	0	0	18.34	15.80	0.220	0.466	0.427	6.58	2.99	0.061	0.065	2.04	1.40	1.66	0.71	8.78	23.16

Appendix IX-1 (continued)

#	st#	Sam#	horizon	shape	size n	part	depth	Mineralogy						Chemistry													
					(cm)			bus.	ver.	qz	ph	pc	sm	Mn	Fe	Cu	Ni	Co	Si	Al	Zn	Pb	Ca	Mg	Na	K	H+	H-
121	3939	FG618	top	ID	2	1 whole		18	9	7	10	0	0	18.11	14.64	0.318	0.607	0.389	6.54	3.07	0.067	0.208	1.83	1.56	1.73	0.88	9.63	20.48
122	3940	FG619	top	S	2	1 1/4		4	14	12	0	0	0	17.32	17.29	0.151	0.370	0.473	5.96	2.55	0.057	0.094	2.06	1.20	1.62	0.64	9.29	23.05
123	3941	FG620	top	S	2	1 1/2		9	13	10	6	0	0	18.16	15.19	0.208	0.471	0.422	6.14	2.84	0.062	0.076	2.10	1.36	1.65	0.77	9.38	22.10
124	3942	FG621	top	ID	3	1 1/2		13	12	9	3	0	7	16.58	14.66	0.294	0.579	0.329	7.40	3.17	0.063	0.068	1.73	1.73	1.76	0.75	8.49	20.36
125	3943	FG622	top	IS	2	1 1/2		10	14	6	4	0	0	18.46	14.55	0.265	0.536	0.378	6.82	3.19	0.067	0.059	2.01	1.46	1.71	0.75	9.38	22.51
126	3944	FG623	top	ID	3	1 1/2		14	9	5	10	0	0	14.76	15.91	0.251	0.486	0.295	8.10	3.39	0.064	0.052	1.76	1.47	1.77	1.01	9.42	20.71
127	3945	FG624	top	IS	3	1 1/4		4	15	15	4	0	0	17.68	15.98	0.192	0.441	0.401	6.13	2.56	0.063	0.063	2.02	1.28	1.65	0.70	9.89	23.42
128	3946	FG625	top	T	2	1 whole		10	10	4	4	0	0	14.84	18.14	0.225	0.415	0.342	6.07	2.81	0.062	0.090	1.81	1.27	1.58	0.71	9.78	21.24
129	3947	FG626	top	IS	2.5	1 1/2		4	11	8	3	0	0	15.40	17.69	0.189	0.379	0.417	6.27	2.82	0.061	0.096	2.10	1.23	1.69	0.68	9.26	22.76
130	3948	FG627	top	S	2.5	1 1/4		5	11	8	4	0	0	16.35	16.57	0.254	0.434	0.424	5.86	2.73	0.062	0.086	2.04	1.25	1.67	0.67	9.23	22.35
131	3949	FG628	top	S	2	1 1/2		5	10	5	3	0	0	15.22	16.06	0.215	0.399	0.393	5.90	2.71	0.056	0.070	2.01	1.17	1.64	0.68	9.70	23.22
132	3950	FG629	top	S	2	1 1/2		8	8	5	0	0	0	17.20	15.30	0.210	0.413	0.401	5.51	2.64	0.056	0.061	2.07	1.18	1.59	0.69	13.31	19.86
133	3951	FG630	top	ID	1-1.5	2 whole		20	10	5	4	0	0	19.46	12.36	0.397	0.773	0.294	6.02	3.25	0.083	0.058	1.97	1.80	1.74	0.84	10.01	19.37
134	3982	B97L	top	SP	4	1 1/8		0	12	0	4	0	0	16.57	18.90	0.137	0.251	0.450	5.03	2.00	0.052	0.089	2.16	1.02	1.57	0.59	8.88	25.09
135		B97M	top	S	2	1 whole		0	11	3	3	0	0	16.67	17.99	0.129	0.275	0.440	5.85	2.44	0.050	0.113	2.42	1.04	1.66	0.74	9.22	24.60
136		B97S	top	ID	1	2 whole		0	12	3	8	0	0	16.05	15.82	0.177	0.333	0.342	6.59	3.21	0.053	0.056	3.16	1.14	1.52	0.76	8.95	22.81
137		B97X	-16cm	IDP	4	1 whole		0	12	0	0	0	0	16.71	19.41	0.123	0.241	0.487	5.04	2.03	0.051	0.108	2.24	1.05	1.55	0.60	9.03	25.73
138	4020	B99	top	IS	1	5 whole		16	9	7	20	0	0	14.77	13.36	0.313	0.591	0.268	8.69	4.14	0.065	0.039	1.69	1.59	1.92	1.51	8.94	17.14
139	4027	B100L	top	S	5	1 whole		0	12	14	10	0	0	17.46	16.43	0.158	0.376	0.478	5.76	2.57	0.054	0.069	2.20	1.20	1.67	0.79	9.89	22.85
140		B100M	top	IS	2	1 whole		7	10	8	0	0	0	16.94	16.54	0.202	0.407	0.451	5.53	2.72	0.059	0.087	2.04	1.26	1.63	0.66	10.56	21.65
141		B100S	top	ID	0.7-1	8 whole		11	9	5	18	0	0	14.42	14.13	0.267	0.403	0.375	8.57	4.19	0.054	0.064	1.86	1.40	1.93	1.28	8.52	20.31
142	3904	P397Top	top	ISP	2	1 whole		10	10	7	5	0	0	16.74	16.08	0.258	0.475	0.416	6.21	3.12	0.066	0.079	2.01	1.53	1.66	0.74	8.25	23.62
143		P397VI	-200cm	X	4	1 whole	0-15mm	0	12	27	15	0	5	14.43	13.65	0.166	0.226	0.356	10.25	4.09	0.038	0.077	2.19	1.13	2.10	1.30	6.93	23.10
144	3906	P398III	-231cm	IDP	1.5	1 1/2		22	10	0	11	0	7	14.32	13.97	0.442	0.591	0.176	10.98	3.58	0.066	0.032	1.39	2.12	1.66	1.21	7.76	14.72
145		P398V	-368cm	F	1	1 1/2		10	9	7	8	0	15	6.44	18.55	0.229	0.243	0.104	13.74	3.83	0.036	0.038	1.02	1.69	1.54	1.47	8.01	14.83
146	3908	P399Top	top	C	0.6	1 top	0-6mm	0	14	8	18	0	0	15.26	16.43	0.123	0.226	0.338	7.67	3.05	0.043	0.102	2.16	1.02	2.05	1.20	8.91	22.57
147		P399VIII	-58cm	ID	3	1 1/2		4	11	4	4	0	0	15.35	18.58	0.157	0.285	0.380	7.47	2.80	0.053	0.094	2.06	1.23	1.68	0.81	6.83	24.28
148	3910	P400Top	top	S	1	1 whole		15	9	10	7	0	0	19.29	13.90	0.343	0.609	0.346	5.99	3.45	0.075	0.067	1.88	1.82	1.59	0.74	9.64	20.99
149		P400V	-43cm	ID	5	1 whole	0-12mm	41	3	8	31	0	0	16.60	4.46	0.731	0.751	0.111	12.00	5.63	0.085	0.002	1.39	1.99	2.70	2.13	7.44	16.51
150	3922	P402Top	top	ID	2	1 1/2		8	10	8	3	0	0	19.89	14.29	0.352	0.608	0.370	5.76	3.14	0.071	0.078	2.03	1.60	1.61	0.74	9.16	22.72

Appendix IX-1 (continued)

#	st#	Sam#	horizon	shape	size n (cm)	part	depth	Mineralogy bus.	ver.	qz	ph	pc	sm	Chemistry Mn	Fe	Cu	Ni	Co	Si	Al	Zn	Pb	Ca	Mg	Na	K	H+	H-
151		P402VI	-270cm	IS	1.5	1 1/2, soft		11	13	20	0	0	7	16.56	15.58	0.256	0.608	0.140	8.16	2.84	0.082	0.062	1.34	1.71	1.47	1.18	8.27	15.67
152	3930	P404Top	top	T	6	1 1/4		7	10	5	16	0	0	15.20	15.59	0.212	0.405	0.319	8.15	3.75	0.057	0.076	1.93	1.62	1.90	1.07	6.95	22.69
153		P404IV	-79cm	IS	1.5	1 1/2, soft		4	15	20	4	0	5	17.55	16.70	0.180	0.374	0.139	7.18	2.35	0.069	0.038	1.61	1.53	1.56	1.03	7.43	17.41
154		P404VI	-155cm	IS	1.5	1 whole, soft		4	14	3	4	0	5	17.08	15.10	0.171	0.452	0.074	8.96	2.97	0.079	0.017	1.67	1.82	1.58	1.43	6.13	22.87
155	3948	P406Top	top	IS	1	1 1/2		8	12	5	5	0	0	19.12	16.72	0.264	0.471	0.466	5.06	2.66	0.063	0.095	1.95	1.45	1.59	0.63	8.20	22.72
156		P406pil	-28cm	F	1	1 whole		8	9	3	3	0	0	18.93	16.97	0.264	0.470	0.520	4.35	2.35	0.060	0.095	1.93	1.40	1.47	0.60	10.08	20.22
157		P406I	-10cm	S	7	1 inside	2-10mm	0	14	12	8	0	0	18.84	15.50	0.177	0.480	0.534	5.99	2.67	0.050	0.070	2.32	1.16	1.84	0.86	5.53	25.46
158		P406VI	-460cm	IS	1.5	1 1/2, soft		0	14	23	10	0	0	19.57	14.41	0.201	0.334	0.552	5.62	2.48	0.055	0.071	2.39	1.19	1.83	0.68	12.02	22.44
159		P406VIII	-662cm	D	2	1 whole, soft		3	15	22	0	0	4	16.60	17.80	0.137	0.314	0.168	6.67	2.46	0.068	0.039	1.67	1.43	1.57	1.02	9.55	25.42
160		P406cc	-757cm	S	2	1 1/2		7	13	10	4	0	0	18.33	16.62	0.192	0.432	0.469	5.30	2.73	0.062	0.080	2.01	1.39	1.67	0.67	9.55	22.20
161	3960	P407Top	top	IS	1.5	1 whole		10	10	5	4	0	0	16.68	17.33	0.225	0.419	0.440	5.20	2.56	0.063	0.091	1.88	1.43	1.58	0.62	9.80	21.19
162		P407VII	-200cm	IS	1.5	1 1/2, soft		11	17	34	0	0	4	16.71	17.16	0.232	0.496	0.111	7.92	2.62	0.076	0.051	1.52	1.62	1.52	1.08	7.77	15.97
163	3990	P409Top	top	IS	1	3 whole		7	10	3	11	0	0	15.62	15.43	0.205	0.382	0.407	8.23	3.49	0.055	0.073	1.93	1.37	1.81	1.12	9.18	21.45
164	3998	P410Top1	top	ID	1.5	1 whole		5	10	15	5	0	0	16.28	18.75	0.219	0.396	0.439	6.05	2.74	0.064	0.088	1.89	1.41	1.64	0.72	8.35	22.79
165		P410Top2	top	T	4	1 top	0-10mm	0	14	10	4	0	0	17.26	19.35	0.252	0.446	0.467	6.28	2.93	0.068	0.095	2.05	1.49	1.68	0.67	7.76	26.18
166	4013	P411Top	top	IS	1.5	1 whole		7	11	5	0	0	0	16.88	17.03	0.132	0.293	0.421	5.15	2.16	0.047	0.092	2.21	1.07	1.72	0.70	9.52	21.76
167	4030	P412Top	top	IS	1.5	1 whole		8	10	5	0	0	0	16.59	17.78	0.197	0.388	0.451	5.66	2.83	0.057	0.099	2.02	1.32	1.57	0.63	9.89	23.24
168		P412II	-135cm	IS	0.8	1 whole, soft		22	14	24	0	0	0	18.99	14.23	0.350	0.930	0.061	5.81	2.88	0.122	0.047	1.28	2.14	1.67	1.10	8.47	12.00
169	4013	FG692	top	S	6	1 inside	nuclei	185	0	0	0	0	0	39.38	2.63	0.171	0.160	0.112	1.11	0.67	0.039	0.029	0.91	1.87	1.21	1.26	7.85	7.16

NOTE. sam#: suffix L=large, M=medium, S=small, T=top, I=inside
horizon: position on/in sediment
shape: S=sherical, D=discoidal, T=tabular, I=irregular, P=polynucleated
n: number of analyzed nodules ,
depth: depth of analyzed part from nodule surface.
mineralogy: expressed as % peak height of 2kcps full scale. They do not represent absolute contents.
bus.=buserite, ver.=vernadite, qz=quartz, ph=phillipsite, pc=plagioclase, sm=smectite
chemistry: in wt. % to 110°C-dried basis. H+=water content. H-=water content to air-dried basis.